P. Suárez-Casal, Ó. Fresnedo, L. Castedo and J. García-Frías, "Analog Transmission of Correlated Sources Over BC With Distortion Balancing," in *IEEE Transactions on Communications*, vol. 65, no. 11, pp. 4871-4885, Nov. 2017, doi: 10.1109/TCOMM.2017.2726065.

Link to published version: https://doi.org/10.1109/TCOMM.2017.2726065

Analog Transmission of Correlated Sources over BC with Distortion Balancing

Pedro Suárez-Casal, Óscar Fresnedo *Member, IEEE*, Luis Castedo, *Senior Member, IEEE*, Javier García-Frías, *Senior Member, IEEE*

***Abstract*—Analog transmission of correlated information over Gaussian Broadcast Channels (BCs) using analog Joint Source Channel Coding (JSCC) is addressed. This communication strategy has attractive advantages such as low complexity, minimal delay, graceful degradation and adaptation to time-varying environments. In this work, we focus on the optimization of parametric continuous mappings that satisfy individual Quality of Service (QoS) requirements over Gaussian BCs. This optimization is based on the balancing of the user distortions to ensure the feasibility of the resulting optimization problems. An analysis of the overall distortion corresponding to the considered mappings is carried out to design algorithms that determine the optimal values for the mappings parameters. Results show that the proposed analog JSCC scheme provides near optimal performance and an adequate balancing of the individual distortions.**

***Index Terms*—Multiuser channels, Broadcast Channels, Correlation, Mean square error methods**

I. Introduction

Broadcast communication is the transmission of information from a central node to several devices using a common channel. Broadcast communication arises in a large number of scenarios such as the downlink of cellular systems, or the communication between the control node and a multitude of sensors in a Wireless Sensor Network (WSN). Traditional approaches to design schemes that reliably transmit the source information over a Broadcast Channel (BC) are based on the source-channel separation [1]. This strategy consists in the separate optimization of the source and channel encoders. In the case of Gaussian BCs with a single transmit antenna, the theoretical optimum sum-rate is achieved by using an orthogonal channel access or with a scheme based on superposition coding [2]. When multiple antennas are available at transmission, the optimal strategy is the non-linear precoding technique known as dirty paper coding [3].

In general, the use of properly optimized schemes based on source-channel separation provides near optimal performance, although they present some limitations. On one hand, since these schemes require long block sizes at both encoders to approach the theoretical bounds, their complexity is high and introduce large latency. On the other, since the encoder rates depend on the channel conditions, these systems need to be redesigned on time-varying environments to adapt the encoders to the fluctuations of the channel conditions. Indeed, this approach is not optimal in general in multiuser scenarios, for example when a source must be reconstructed by multiple users with different distortions [4], [5].

An alternative strategy consists in the join optimization of the source and channel encoders into a a single operation. The transmission of correlated sources over BCs using Joint Source Channel Coding (JSCC) techniques has already been studied in several works. The optimization of a bipartite graph to randomly map the source encoder outputs to the channel encoder inputs is stated in [6] to ensure the reliable communication of pairs of correlated samples to two receivers over BCs. In [7], the same communication problem is addressed considering an external interference which is known at the transmitter and is correlated with the source symbols. In this work, inner and outer bounds for this scenario are derived, and the design of parametric and non parametric mappings to achieve such bounds is studied. The use of Hybrid Digital Analog (HDA) schemes based on the JSCC approach is also proposed in [8], [9] for the transmission of bivariate Gaussian sources over bandwidth mismatch BCs. The use of JSCC techniques has been shown to achieve the optimal performance also in broadcast networks where two different encoders send correlated information to several receivers [10].

When the source information is analog, discrete-time continuous-amplitude samples of the original signal can be transmitted using analog JSCC techniques. These techniques are based on the design of continuous space-filling curves that are employed to map the source symbols into the corresponding channel symbols according to a mapping function [11], [12], [13], [14]. Over the last years, analog JSCC mappings have been applied to multiple scenarios such as AWGN and fading channels [15], [16], MIMO systems [17], multiuser communications [18], [19] and network coding [20].

In this work, we address the BC transmission of analog correlated data to two receivers using analog JSCC mappings. In particular, we focus on the design of 2:1 parametric mappings to satisfy individual distortion requirements. In general, the use of parametric mappings has two main advantages with respect to the non parametric ones: 1) low-complexity decoding strategies can be employed at the receivers; and 2) the space-filling curve for the mapping operation can be adapted to the variations of the channel conditions by updating its parameters. For parametric mappings, the distortion after decoding the received symbols can be expressed as a function of its parameters and, therefore, they can be conveniently optimized depending on the goal of the BC communication: minimum sum-distortion, individual distortion targets, max-

Pedro Suárez-Casal, Óscar Fresnedo and Luis Castedo are with the Department of Electronics and Systems, University of A Coruña, 15071, A Coruña, Spain, e-mail: {pedro.scasal, oscar.fresnedo, luis}@udc.es.

Javier García-Frías is with Department of Electrical Engineering, University of Delaware, USA, e-mail: jgf@udel.edu

min fairness, balancing of the user distortions, etc. In this paper, we focus on the last criterion since the idea of distortion balancing ensures the feasibility of the resulting optimization problems [21]. In particular, two different analog JSCC mappings are considered depending on the SNR regime. On one hand, given that uncoded schemes have been shown to achieve the optimal performance for low SNR values for multiuser communications [18], we study the optimization of these mappings to support the balancing of the user distortions. On the other, low-complexity parametric mappings based on sinusoidal functions [22] are employed in the high SNR regime.

The main contributions of this work are summarized as follows:

- Sine-like mappings are updated to satisfy individual targets and to support the distortion balancing when correlated data is sent over Additive White Gaussian Noise (AWGN) BCs. The proposed transformation of the original mapping is based on incorporating an additional parameter to satisfy the individual distortion requirements.
- The distortion obtained after decoding the received symbols when using sine-like mappings is mathematically analyzed for the case of bivariate Gaussian sources and AWGN channels. As a result, an approximation of the actual distortions is presented and employed to optimize the mapping parameters for different scenarios using a searching algorithm.
- A systematic optimization for the parameters of the uncoded scheme is proposed for the scenarios of interest, where the goal is the balancing of the individual distortions.

II. System Model

Let us consider the transmission of analog correlated information over a Gaussian BC using analog JSCC mappings. In particular, we focus on the two-user case where the real-valued source symbols $\mathbf{x} = [x_1 \ x_2]^T$ are assumed to follow a bivariate Gaussian distribution, i.e. $\mathbf{x} \sim \mathcal{N}(\mathbf{0}, \mathbf{C}_x)$ with a covariance matrix $\mathbf{C}_\mathbf{x} = [1 \ \rho; \rho \ 1]$. The probability density function (pdf) of $\mathbf{x}$ is given by

$$p_\mathrm{x}(\mathbf{x}) = \frac{1}{\sqrt{(2\pi)^2 \det\{\mathbf{C}_\mathbf{x}\}}} \exp\left(-\frac{1}{2}\mathbf{x}^T \mathbf{C}_\mathbf{x}^{-1}\mathbf{x}\right). \quad (1)$$

Each pair of source symbols is first encoded by a 2:1 analog encoder $g(\cdot): \mathbb{R}^2 \to \mathbb{R}$, and the resulting symbol is then transmitted to the two users over the BC. Hence, the received signal can be expressed as

$$\mathbf{y} = g(\mathbf{x})\mathbf{1} + \mathbf{n}, \quad (2)$$

where $\mathbf{y} = [y_1 \ y_2]^T \in \mathbb{R}^2$ stacks the received symbols of the two users, $\mathbf{1}$ is the 2×1 vector of ones, and $\mathbf{n} = [n_1 \ n_2]^T \in \mathbb{R}^2$ represents the AWGN at the receivers, with $\mathbf{n} \sim \mathcal{N}(\mathbf{0}, \mathbf{C}_n)$ and $\mathbf{C}_n = \mathrm{diag}\left(\sigma_{n,1}^2, \sigma_{n,2}^2\right)$. A global power constraint is imposed at the transmitter, and therefore the encoding function must be designed to satisfy the constraint $\mathbb{E}[g^2(\mathbf{x})] \leq P$.

At each user, an estimate of its source symbols is calculated from the received symbol as $\hat{x}_i = h_i(y_i), \ i = 1,2$, with $h_i(\cdot)$ the decoding function of each user. The distortion between source and estimated symbols is measured according to the Mean Squared Error (MSE) criterion as

$$\xi_i = \mathbb{E}\left[|x_i - \hat{x}_i|^2\right] \quad i = 1,2. \quad (3)$$

In this work, we explore the analog transmission of the source information over Gaussian BCs using analog JSCC mappings. Such mappings are designed to satisfy a pair of individual distortion targets such that $\xi_i \leq \varepsilon_i$, where ε_i represents the distortion target for the i-th user.

$$\min_{g(\cdot),h_1(\cdot),h_2(\cdot)} \ \xi_i, \quad s.t. \ \mathbb{E}[g^2(\mathbf{x})] \leq P, \ \xi_i \leq \varepsilon_i, \quad i = 1,2, \quad (4)$$

This problem is feasible as long as the distortion targets ε_i lie on the region of achievable distortions, given a transmit power P and noise variances $\sigma_{n,1}^2$ and $\sigma_{n,2}^2$. To guarantee its feasibility, (4) can be reformulated as a balancing problem to satisfy scaled versions of the original targets that lie on the region of achievable distortions, i.e.,

$$\min_{g(\cdot),h_1(\cdot),h_2(\cdot)} \ b, \quad s.t. \ \mathbb{E}[g^2(\mathbf{x})] \leq P, \ \xi_i - b\varepsilon_i \leq 0, \quad i = 1,2, \quad (5)$$

where b is a real-valued balancing level and $b\varepsilon_i$ represents a balanced version of the original targets. Without loss of generality, we address those cases where the distortion target for the first user is lower than that of the second user, i.e., $\varepsilon_1 \leq \varepsilon_2$.

A. Distortion bound

The optimal performance of analog systems is given by the optimal cost-distortion tradeoff, known as the Optimum Performance Theoretically Attainable (OPTA). In the considered scenario, we define a distortion bound for the balancing problem based on the characterization for the region of achievable distortion for the transmission of bivariate Gaussian sources over BCs [23] .

As mentioned in the previous section, we focus on analog schemes that satisfy individual distortion targets with an appropriate balancing level. Therefore, given a pair of initial targets ε_1 and ε_2, all the elements of the set of achievable distortions that satisfy the balancing criterion are always related by the ratio $k = \varepsilon_2/\varepsilon_1$. Hence, we restrict the calculation of the optimal bound to those scenarios where $\varepsilon_2 = k\varepsilon_1$. Since we assume $\varepsilon_2 \geq \varepsilon_1$, we have $k \geq 1$.

Let (D_1, D_2) be a pair of achievable distortions under a given power constraint P, and denote its collection as $\mathscr{D}(P, \rho, \sigma_{n_1}, \sigma_{n_2})$. From the inner bound for the region of achievable distortions given in [23], and assuming the distortion pairs that satisfy that $D_2 = kD_1$, the achievable distortion for the first user can be written piecewise as in (6). There $D_1^u(P, \rho, \sigma_{n_1}, \sigma_{n_2}, k)$ represents the distortion obtained with the optimal uncoded scheme for a given k, and D_2^+ delimits the distortion for the second user from which the uncoded scheme is no longer the optimal transmission strategy [23, Eq. (16)]

$$D_2^+ = \frac{(P + 2\sigma_{n_2})(1-\rho^2) + \sqrt{(P^2 - (P+2\sigma_{n_2})^2\rho^2)(1-\rho^2)}}{2(P+\sigma_{n_2})}.$$

$$D_1^{\text{opt}}(P,\rho,\sigma_{n_1}^2,\sigma_{n_2}^2,k)=\begin{cases}\frac{\sigma_{n_1}^2}{P+\sigma_{n_1}^2}, & P\le w(\rho,\sigma_{n_1}^2,\sigma_{n_2}^2,k)\\ D_1^u(P,\rho,\sigma_{n_1}^2,\sigma_{n_2}^2,k), & P\le \frac{2\rho\sigma_{n_2}^2}{1-\rho} \text{ or } D_1^u\ge\frac{D_2^+}{k}\\ \frac{\sigma_{n_2}^2-\sigma_{n_1}^2+\sqrt{\left(\sigma_{n_2}^2-\sigma_{n_1}^2\right)^2+4k\sigma_{n_1}^2\left(P+\sigma_{n_2}^2\right)\left(1-\rho^2\right)}}{2k\left(P+\sigma_{n_2}^2\right)} & P>\frac{2\rho\sigma_{n_2}^2}{1-\rho} \text{ and } D_1^u<\frac{D_2^+}{k}\end{cases} \tag{6}$$

$$w(\rho,\sigma_{n_1}^2,\sigma_{n_1}^2,k)=\frac{-\sigma_{n_2}^2-(1-\rho^2-k)\sigma_{n_1}^2+\sqrt{\left(\sigma_{n_2}^2-(1-\rho^2-k)\sigma_{n_1}^2\right)^2-4k\rho^2\sigma_{n_1}^2\sigma_{n_2}^2}}{2(1-\rho^2)} \tag{7}$$

$$D_1^{\text{opt}}(k,\rho,\eta)=\begin{cases}\frac{1}{1+\eta}, & \eta\le\frac{k-1}{1-\rho^2}\\ \frac{(1+k)\left(1-\rho^2\right)(2+\eta)-2\rho\sqrt{k\eta^2\left(1-\rho^2\right)^2-(1-k)^2(1+\eta)\left(1-\rho^2\right)}}{(1+\eta)\left((1+k)^2-4\rho^2k\right)}, & \frac{k-1}{1-\rho^2}\le\eta<u(\rho,k)\\ \sqrt{\frac{1-\rho^2}{k(1+\eta)}}, & \eta\ge u(\rho,k)\end{cases} \tag{8}$$

This expressions simplify for symmetric BCs when $\sigma_n^2=\sigma_{n,1}^2=\sigma_{n,2}^2$. In this case, the minimum distortion achievable for the first user is given by (8), where $\eta=P/\sigma_n^2$ represents the Signal-to-Noise Ratio (SNR) value for both users, and the threshold $u(\rho,k)=v(\rho,k)+\sqrt{v(\rho,k)(v(\rho,k)-1)}$, with $v(\rho,k)=\frac{k^2+2k\rho+1}{2k(1-\rho^2)}-1$, is determined by equating the distortion in the third region to D_2^+/k and solving for η. As observed, the SNR region is split into three different intervals: $\mathscr{D}_1=\left\{\eta\mid\eta\le\frac{k-1}{1-\rho^2}\right\}$, $\mathscr{D}_2=\left\{\eta\mid\frac{k-1}{1-\rho^2}\le\eta<u(\rho,k)\right\}$ and $\mathscr{D}_3=\{\eta\mid\eta\ge u(\rho,k)\}$.

The achievable distortions for the second user in the region $\mathscr{D}_2\cup\mathscr{D}_3$ is the distortion of the first user scaled by the factor k, while the region $\mathscr{D}_1$ corresponds to transmit only the source of the first user [18]. In this case, the distortion for the second user is the error variance obtained with the linear Minimum Mean Squared Error (MMSE) filter, since the source symbols are Gaussian distributed. Thus, the distortion ratio is lower than or equal to k, and larger distortions could only be obtained for the second user by penalizing the decoding. As a consequence, the corresponding SNR interval is not interesting in terms of distortion balancing or design of coding schemes to satisfy distortion targets. The achievable distortion for the second user is hence

$$D_2^{\text{opt}}(k,\rho,\eta)=\begin{cases}1-\frac{\rho^2\eta}{1+\eta}, & \eta\le\frac{k-1}{1-\rho^2}\\ \min\{1,kD_1^{\text{opt}}\}, & \eta>\frac{k-1}{1-\rho^2}\end{cases} \tag{9}$$

III. Analog JSCC Mappings

Two types of analog mappings are considered along this work: uncoded and sine-like. Uncoded mappings are helpful in the low SNR regime whereas sine-like mappings will be used for high SNRs. Both mappings compress two source symbols into one channel symbol sent over the BC.

A. Uncoded Mappings

When $(D_1,D_2)\in\mathscr{D}_1\cup\mathscr{D}_2$, i.e. $\eta<u(\rho,k)$, the minimum distortion $(D_1^{\text{opt}},D_2^{\text{opt}})$ is achieved with an uncoded scheme that consists of a linear combination of the source symbols [18], i.e.,

$$g^u(\mathbf{x})=\sqrt{\frac{P}{m^2+n^2+2\rho mn}}\,(mx_1+nx_2)=\mathbf{v}^T\mathbf{x}, \tag{10}$$

with m and n real-valued mapping parameters, and $\mathbf{v}=\sqrt{\frac{P}{m^2+n^2+2\rho mn}}[m\ n]^T$. These parameters must be optimized for each SNR region in (8) as we will explain in Section IV.

The optimal decoder for this setup is the linear MMSE estimator, i.e.

$$h_i^u(y_i)=\left[\mathbf{C}_{\mathbf{x}}\mathbf{v}(\mathbf{v}^T\mathbf{C}_{\mathbf{x}}\mathbf{v}+\mathbf{C}_n)^{-1}y_i\right]_i,\quad i=1,2. \tag{11}$$

The resulting expected individual distortions are given by [18], [24]

$$\xi_1^u(m,n,\eta_1)=\frac{1}{(1+\eta_1)^2}+\frac{\eta_1^2n^2(1-\rho^2)+\eta_1(m^2+n^2(2-\rho^2)+2\rho mn)}{(1+\eta_1)^2(m^2+n^2+2\rho mn)} \tag{12}$$

$$\xi_2^u(m,n,\eta_2)=\xi_1^u(n,m,\eta_2), \tag{13}$$

where $\eta_1=P/\sigma_{n_1}^2$ and $\eta_2=P/\sigma_{n_2}^2$ represent the individual SNRs.

B. Sine-like Mappings

Sine-like mappings arise from a parametric approximation to the non-parametric analog JSCC mappings for the considered scenario. Such non-parametric mappings and their corresponding decoder can be obtained by means of multiple techniques such as steepest descent [25], vector quantization [26], or deterministic annealing [19]. For example, in the steepest descent approach, the analog encoder and decoder are alternatively optimized to decrease the MSE. For given enconder $g(\cdot)$, the optimal MMSE decoder can be calculated as follows

$$h_i^{\text{MMSE}}(y_i)=\mathbb{E}[\mathbf{x}|y_i]=\frac{\int\mathbf{x}\ p_x(\mathbf{x})\ p_{n_i}(y_i-g(\mathbf{x}))\ \mathrm{d}\mathbf{x}}{\int p_x(\mathbf{x})\ p_{n_i}(y_i-g(\mathbf{x}))\ \mathrm{d}\mathbf{x}}, \tag{14}$$

where $p_{n_i}(n) = (2\pi\sigma_{n_i}^2)^{-1/2}\exp\left(-n^2/\sigma_{n_i}^2\right)$ represents the pdf of the Gaussian noise distribution. The optimal encoder, however, cannot be expressed in terms of the decoder in a closed-form. It can be determined by means of a steepest descent search on the domain of the encoding functions to minimize the MSE for a given decoder, subject to a power constraint [25]. Although providing good performance, non parametric approaches suffer from high computational cost and their solutions are specific to the conditions of each scenario. Thereby, if noise variance or source correlation change, new encoding and decoding functions have to be found.

Parametric approaches to analog JSCC are an appealing alternative where the encoder and the decoder are expressed as functions of some parametrized space-filling curve. This structure allows low complexity implementations of the decoder and the adaptation of the encoder parameters to the channel conditions. The parametric mapping proposed in [22] for single-user scenarios can be adapted to the Gaussian BC with individual distortions as

$$\mathbf{c}_{\alpha,\Delta,\beta}(t) = \mathbf{U}\Sigma^{1/2}\begin{pmatrix} 1 & \sqrt{\frac{\lambda_2}{\lambda_1}}\beta \\ 0 & 1 \end{pmatrix}\mathbf{s}(t), \tag{15}$$

where

$$\mathbf{s}(t) = [s_x(t)\ s_y(t)]^T = \begin{pmatrix} t - \frac{1}{2\alpha}\sin(2\alpha t) \\ \Delta\sin(\alpha t) \end{pmatrix}, \tag{16}$$

and $\mathbf{C_x} = \mathbf{U}\Sigma\mathbf{U}^H$ is the eigenvalue decomposition of the source covariance, with $\Sigma = \mathrm{diag}(\lambda_1,\lambda_2)$ the matrix containing the eigenvalues and $\lambda_1 \geq \lambda_2$. Hence, the matrix $\mathbf{U}\Sigma^{1/2}$ projects the parametric curve on the source space. Compared to the parametric curve for single-user 2:1 compression, (15) adds a new parameter β to support the balancing of individual distortions. The choice of $\mathbf{s}(t)$ is motivated as an approximation to the non-parametric mappings obtained with the steepest-descent algorithm explained previously, and after analyzing other mappings proposed for the BC scenario [7], [27].

Different approaches can be considered to map the source symbols into the parametric curve. The conventional one is the Minimum Distance (MD) mapping which consists in finding the point on the curve with minimum Euclidean distance to the source symbols $\mathbf{x} = [x_1, x_2]$. The encoded symbol is thus obtained as $g^m(\mathbf{x}) = \arg\min_t \ \|\mathbf{x} - \mathbf{c}(t)\|^2$.

For symmetrical BCs, an alternative is the Expected Distortion (ED) mapping. Indeed, assuming that a ML decoder will be used, the encoding process may take into account the effect of the AWGN channel as

$$g^e(\mathbf{x}) = \arg\min_t \ \int \|\mathbf{x} - \mathbf{c}(t)\|^2 p_n(n-t)\mathrm{d}n. \tag{17}$$

The optimal strategy to decode the source symbols at each user is the MMSE estimator given by (14). However, the computational complexity of this solution is large because it requires numerical calculation of the integrals in (14). A lower complexity alternative is the Maximum Likelihood (ML) decoder that can be implemented as

$$h_i^{\mathrm{ML}}(y_i) = \left[\mathbf{c}_{\alpha,\Delta,\beta}(y_i)\right]_i, \quad i = 1,2. \tag{18}$$

In addition, previous works have shown that a two-stage receiver can improve the performance of ML decoding, with negligible impact on the computational complexity, by chaining it with the linear MMSE decoder [28]. This decoder can be expressed as

$$h_i^{\mathrm{two}}(y_i) = \left[\mathbf{c}_{\alpha,\Delta,\beta}\left(\frac{y_i}{1+\sigma_{n_i}^2}\right)\right]_i, \quad i = 1,2. \tag{19}$$

The observed symbols at each user are first filtered with the linear MMSE filter to mitigate the impact of the noise, and the resulting symbols are then decoded according to an ML strategy.

IV. Optimization of mapping parameters

Both uncoded and parametric sine-like analog JSCC schemes require an optimization of the mapping parameters to satisfy the individual distortion targets. In the ensuing sections, an expression of the user distortions depending on the mapping parameters is first obtained for uncoded and sine-like mappings. The obtained expressions are then employed to optimize the mapping parameters according to the distortion targets and the channel conditions.

A. Uncoded Mapping

The expected distortion when uncoded mappings are used is given by (12) and (13). We are interested in obtaining the parameters m and n that satisfy $\xi_2^u(m,n,\eta_1)/\xi_1^u(m,n,\eta_2) = k$. This mapping is able to achieve the optimal performance bound in (6) when the SNR is in the first two intervals.

The first SNR interval is only defined when the user distortion targets are strictly different ($k > 1$). In this case, the optimal parameters of the uncoded scheme are $m = 1$ and $n = 0$ which corresponds to transmitting only the symbol to the first user. As a consequence, the achievable distortion for the second user does not meet the ratio defined above and is directly determined by the error variance of the MMSE estimator.

In the second SNR interval, the optimal parameters can be obtained from the distortions of the uncoded scheme in (12) and (13). After equating $\xi_2^u(m,n,\eta_2) = k\xi_1^u(m,n,\eta_1)$ and solving for n we obtain

$$n = \frac{-\rho z + \sqrt{\rho^2 z^2 - (z+\eta_2(1-\rho^2))(z-\eta_1(z-1)(1-\rho^2))}}{z+\eta_2(1-\rho^2)}m, \tag{20}$$

where $z = 1 - k\frac{1+\eta_2}{1+\eta_1}$, for any $m > 0$.

B. Sine-like mappings

As shown in [22], the encoder parameters of sine-like mappings (α, Δ) can be optimized by using an approach based on a least squares fitting of the non-parametric curves obtained in Section III-B [24]. The optimal values of the parameters are chosen so that the resulting parametric mapping accurately matches the non-parametric curve. However, this approach cannot be considered for scenarios with asymmetric distortion requirements because non-parametric mappings were not obtained in such cases. A more generic approach is to determine the user distortions as a function of the encoder parameters. Due to the difficulty to obtain exact expressions,

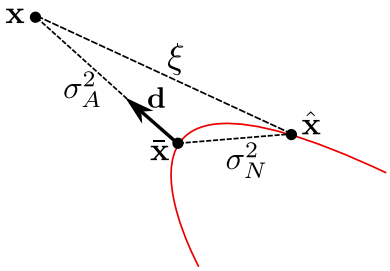

Fig. 1. Components of the total error ξ with ML decoder given the mapping error σ_A^2 and the noise error σ_N^2.

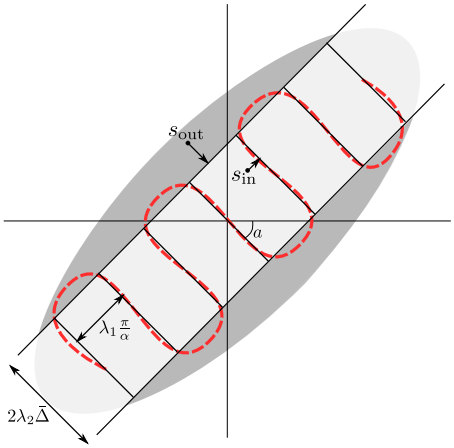

Fig. 2. Approximation of the sinusoid mapping. The dashed red line represents the parametric curve used by the encoder. The black lines represent the approximation of the mapping.

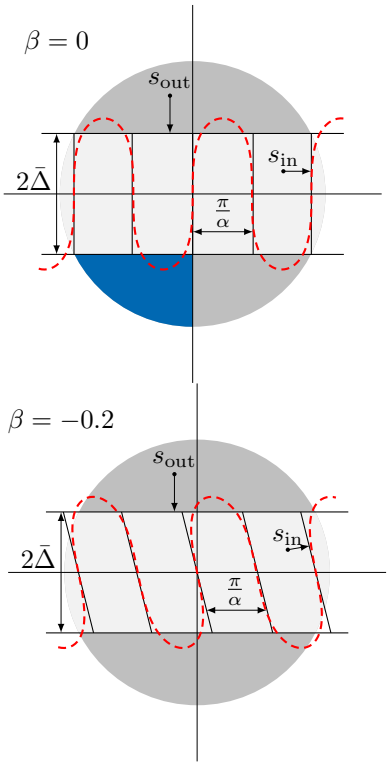

Fig. 3. Equivalent sine-mapping and the approximation one before the projection on the source space.

we assume different approximations to make the calculation of the estimate errors affordable.

The distortion of any parametric encoder assuming ML decoding can be decomposed into three components. The first is the mapping error, and it is related to the mapping from the source symbol to the space-filling curve, the second is related to the channel distortion on the transmitted symbol, and the third appears when these two errors are not orthogonal [15]. This is shown in Figure 1 when a source symbol $\mathbf{x}$ is encoded using the parametric sine-like mapping, is transmitted over an AWGN channel and is decoded with an ML approach. Mathematically, denoting $\bar{x}_i$ as the point on the curve where the source symbol for the i-th user is mapped, the individual distortions can be expressed as

$$\xi_i^{\text{sin}} = \mathbb{E}\left[\left((x_i-\bar{x}_i)-(\hat{x}_i-\bar{x}_i)\right)^2\right] = \sigma_{A,i}^2+\sigma_{N,i}^2-\gamma_i, \qquad (21)$$

where $\sigma_{A,i}^2 = \mathbb{E}\left[(x_i-\bar{x}_i)^2\right]$ is the mapping error, $\sigma_{N,i}^2 = \mathbb{E}\left[(\hat{x}_i-\bar{x}_i)^2\right]$ is the channel error, and $\gamma_i = 2\mathbb{E}\left[(\hat{x}_i-\bar{x}_i)(x_i-\bar{x}_i)\right]$ is a residual term motivated because the mapping error and the channel error are not necessarily orthogonal on the curve, as shown in Figure 1. In the ensuing paragraphs, approximations of these three errors for sinusoidal mappings are developed.

1) Mapping Error: An approximation of this error can be computed from a simplified version of the proposed sine-like mapping. As shown in Figure 2, the source space is split into two regions, a rectangular one (light grey) and the remaining region (dark grey). In the original mapping, represented by the red dashed curve, the points of the source space that lie on the outer region (dark grey) are assumed to be mapped to the lobes of the curve. The points on the inner rectangular region are assumed to be mapped to the straight parts. Hence, the overall error due to the mapping operation can be approximated by the sum of the MSE corresponding to each of these regions.

An interesting simplification is that the errors for the inner and outer regions can be computed before the projection of the mapping on the source space. The resulting errors are then multiplied by the eigenvalues of the covariance matrix, λ_1 and λ_2, to fit the actual mapping error after the projection. The equivalent scenario disregarding the mapping projection is illustrated in Figure 3. The left side of the figure represents the mapping when $\beta = 0$ and, therefore, the mapping is not tilted with respect to the vertical axis. In the right side, a version of the mapping with a certain tilt degree given by β is plotted.

An important issue to obtain an accurate estimate of the components for the mapping error is to properly adjust the height of the outer rectangle, since the width of the inner rectangles corresponds to half of the sinusoid period π/α. The height of this rectangle is defined as $2\bar{\Delta}$, where the parameter $\bar{\Delta}$ is a function of the original Δ in the parametric mapping. We have determined this parameter by finding the point $\bar{t}$ on the curve whose slope is larger than a given threshold U, and evaluated the second component of the mapping in that point.

Thus,

$$\frac{\mathrm{d}s_x(\bar{t})}{\mathrm{d}s_y(\bar{t})} = \frac{1-\cos(2\alpha\bar{t})}{\Delta\alpha\cos(\alpha\bar{t})} = U, \tag{22}$$

$$\bar{\Delta} = \Delta\sin(\alpha\bar{t}) \tag{23}$$

As observed in Figure 2, we seek to identify those cut points on the curve where the mapping shape changes from the straight part to the curved shape. As explained in Appendix A, after solving the above equations, we obtain

$$\bar{\Delta} = \frac{U\alpha\Delta^2}{4}\sqrt{-2+2\sqrt{1+\left(\frac{4}{U\alpha\Delta}\right)^2}}. \tag{24}$$

The threshold U can be selected experimentally to ensure a right approximation.

Once the dimensions of the rectangular mapping are established, we determine an approximation for the errors corresponding to the inner and outer regions using the alternative mapping. On the one hand, the error of the points inside the rectangle can be approximated by the error of a scalar quantizer with an interval size π/α. Thus,

$$e_{\text{in}} = \frac{\pi^2}{12\alpha^2} \tag{25}$$

On the other hand, the MSE for the points outside the rectangle is obtained assuming that such points are mapped to the closest point on the corresponding edge of the rectangle. In this case, the error can be computed as the variance of the points that lie outside the rectangle with respect to $\bar{\Delta}$ or, equivalently, as the variance of a circularly symmetric Gaussian truncated to that region. As observed in Figure 3 (left side), this variance is exactly the same for the four quadrants on the 2D plane. Hence, we can calculate it on the quadrant highlighted in blue as

$$e_{\text{quad}} = \frac{1}{2\sigma_x^2\pi}\int_{-\infty}^{-\bar{\Delta}}\int_{-\infty}^{0}|x_2+\bar{\Delta}|^2\exp\left(-\frac{x_1^2+x_2^2}{2\sigma_x^2}\right)\mathrm{d}x_1\,\mathrm{d}x_2, \tag{26}$$

and then the outer error will be $e_{\text{out}} = 4e_{\text{quad}}$. Solving the integral in (26) and rearranging the resulting terms, we obtain the following expression

$$e_{\text{out}} = (1-p_{\text{in}})(1+\bar{\Delta}^2) - \frac{2\bar{\Delta}}{\sqrt{2\pi}}\exp\left(\frac{-\bar{\Delta}^2}{2}\right) \tag{27}$$

for the error in the outer region, where $p_{\text{in}} = \int_{-\infty}^{\infty}\int_{-\bar{\Delta}}^{\bar{\Delta}} p_x(\mathbf{x})\mathrm{d}\mathbf{x} = \mathrm{erf}\left(\frac{\bar{\Delta}}{\sqrt{2}}\right)$ is the probability that a source point lies inside the considered rectangle with $\mathrm{erf}(x) = \frac{2}{\pi}\int_0^x \exp(-t^2)\mathrm{d}t$ the error function. The steps to arrive at the above expression departing from (26) are detailed in Appendix B.

Finally, the overall mapping error for each user is given by

$$\sigma_{A,1}^2 \approx \lambda_1\cos^2(a)e_{\text{in}}p_{\text{in}} + \frac{\lambda_2}{2}e_{\text{out}} \tag{28}$$

$$\sigma_{A,2}^2 \approx \lambda_1\sin^2(a)e_{\text{in}}p_{\text{in}} + \frac{\lambda_2}{2}e_{\text{out}}, \tag{29}$$

where e_{out} and e_{in} represent the mapping error corresponding to the outer and inner regions, respectively; and the angle $a = \tan^{-1}\left(\frac{\beta-1}{\beta+1}\right)$ represents the slope of the parametric curve depending on the β values. The factors $\cos^2(a)$ and $\sin^2(a)$ are employed to assign the contribution of the points inside the rectangle to the error of each user depending on the mapping tilt degree, and they come from basic trigonometric relationships. However, the contribution of the outer error to the mapping error of each user only depends on the parameter $\bar{\Delta}$. As observed in Figure 3, this contribution for both users is precisely half of the outer error, i.e. $e_{\text{out}}/2$, regardless of the tilt degree. Finally, the eigenvalues λ_1 and λ_2 are necessary to reflect the effect of the projection.

The error expressions in (28) and (29) implicitly depend on the parameter β through the angle a. When $\beta = 0$, this angle is $a = \pi/4$ and, therefore, the terms depending on β simplify to $\cos^2(a) = \sin^2(a) = 1/2$. As expected, the mapping error is the same for both users in this case.

2) Channel Error: Assuming ML decoding, the components of the error due to the channel distortion can be computed as

$$\begin{aligned}\sigma_{N,i}^2 &= \int p_t(t)\int p_{n_i}(n)\left|[\mathbf{c}(t)]_i - h_i^{\text{ML}}(t+n)\right|^2\mathrm{d}n\,\mathrm{d}t \\ &= \int p_t(t)\int p_{n_i}(n)\left|[\mathbf{c}(t)]_i - [\mathbf{c}(t+n)]_i\right|^2\mathrm{d}n\,\mathrm{d}t \\ &= \int A_i(t)p_t(t)\mathrm{d}t,\end{aligned} \tag{30}$$

where $p_t(t)$ and $p_{n_i}(n)$ are the pdf of the mapping output and the i-th component of the noise, respectively; and $\mathbf{c}(t)$ represents the point on the parametric curve given by t. Note that the channel noise moves the encoded symbols only along the curve and, therefore, $\mathbf{c}(t+n)$ corresponds to the symbol at the channel output perturbed by the noise. The $A_i(t)$ terms can be expressed for the sine-like mapping as

$$A_1(t) = \int p_{n_1}(n)|c_x(t) - c_x(t+n)|^2\mathrm{d}n \tag{31}$$

$$A_2(t) = \int p_{n_2}(n)|c_y(t) - c_y(t+n)|^2\mathrm{d}n. \tag{32}$$

where the functions $c_x(t)$ and $c_y(t)$ provide the x and y coordinates of t on the bidimensional space and, therefore, the terms $A_1(t)$ and $A_2(t)$ represent the channel error at the point t for the first and second user, respectively.

Since the eigenvectors of the considered correlation model are $\mathbf{U} = \left[\frac{1}{\sqrt{2}}\frac{1}{\sqrt{2}}; \frac{1}{\sqrt{2}}\frac{-1}{\sqrt{2}}\right]$, and λ_1 and λ_2 are the corresponding eigenvalues, the functions $c_x(t)$ and $c_y(t)$ can be written as

$$c_x(t) = \sqrt{\frac{\lambda_1}{2}}s_x(t) + \sqrt{\frac{\lambda_2}{2}}(1+\beta)s_y(t) \tag{33}$$

$$c_y(t) = \sqrt{\frac{\lambda_1}{2}}s_x(t) - \sqrt{\frac{\lambda_2}{2}}(1-\beta)s_y(t). \tag{34}$$

Replacing (33) and (34) into (31), the expression for the first user error at a point t is

$$\begin{aligned}A_1(t) = \int p_{n_1}(n)\Bigg(&\frac{\lambda_1}{2}|s_x(t)-s_x(t+n)|^2 + \frac{\lambda_2}{2}(1+\beta)^2|s_y(t)-s_y(t+n)|^2 \\ &+\sqrt{\lambda_1\lambda_2}(1-\beta)^2(s_x(t)-s_x(t+n))(s_y(t)-s_y(t+n))\Bigg)\mathrm{d}n\end{aligned}$$

Given that $\mathbb{E}_n[(s_x(t)-s_x(t+n))(s_y(t)-s_y(t+n))]=0$, the third term in the above equation can be disregarded and the expression simplifies to

$$A_1(t)=\int p_{n_1}(n)\left(\frac{\lambda_1}{2}|s_x(t)-s_x(t+n)|^2+\frac{\lambda_2}{2}(1+\beta)^2|s_y(t)-s_y(t+n)|^2\right)\mathrm{d}n$$
$$=\frac{\lambda_1}{2}e_{x_1}(t)+\frac{\lambda_2}{2}(1+\beta)^2e_{y_1}(t). \quad (35)$$

A similar expression is obtained for the second user channel error

$$A_2(t)=\int p_{n_2}(n)\left(\frac{\lambda_1}{2}|s_x(t)-s_x(t+n)|^2+\frac{\lambda_2}{2}(1-\beta)^2|s_y(t)-s_y(t+n)|^2\right)\mathrm{d}n$$
$$=\frac{\lambda_1}{2}e_{x_2}(t)+\frac{\lambda_2}{2}(1-\beta)^2e_{y_2}(t), \quad (36)$$

with

$$e_{x_i}(t)=\sigma_{n_i}^2\left(1-2\cos(2\alpha t)\exp\left(-2\alpha^2\sigma_{n_i}^2\right)\right)+\frac{1}{4\alpha^2}(1-\exp(-2\alpha^2\sigma_{n_i}^2))+\frac{1}{4\alpha^2}\cos(4\alpha t)\left(\exp\left(-2\alpha^2\sigma_{n_i}^2\right)-\frac{1}{2}\exp(-8\alpha^2\sigma_{n_i}^2)-\frac{1}{2}\right)$$

$$e_{y_i}(t)=\Delta^2\left(1-\exp\left(-\frac{\alpha^2\sigma_{n_i}^2}{2}\right)+\cos(2\alpha t)\left(\exp\left(-\frac{\alpha^2\sigma_{n_i}^2}{2}\right)-\frac{1}{2}\exp(-2\alpha^2\sigma_{n_i}^2)-\frac{1}{2}\right)\right).$$

The steps to obtain $e_{x_i}(t)$ and $e_{y_i}(t)$ are developed in the Appendix C.

Notice that equations (35) and (36) corresponding to the channel error for the two users explicitly depend on t. The next step is the integration of these channel errors along all points on the curve according to (30), i.e. $\sigma_{N,1}^2=\mathbb{E}_t[A_1(t)]$ and $\sigma_{N,2}^2=\mathbb{E}_t[A_2(t)]$. However, the pdf of the mapping output $p_t(t)$ cannot be expressed in a closed form and, consequently, the integral in (30) must be calculated numerically. Alternatively, we rely on the relation $\min\{f(x)\}\le\mathbb{E}[f(x)]\le\max\{f(x)\}$. Hence, the expectation of a function $f(x)$ can be approached with a convex combination of the two extreme points as

$$\mathbb{E}[f(x)]=u\max\{f(x)\}+(1-u)\min\{f(x)\}, \quad (37)$$

by selecting a proper value for $u\in[0,1]$.

As an example, Figure 4 plots the error functions $e_{x_i}(t)$ and $e_{y_i}(t)$ for a scenario where a bivariate Gaussian with correlation factor $\rho=0.9$ is mapped using a particular sine-like mapping ($\alpha=10;\ \Delta=1.4;\beta=0$). As observed, $e_x(t)$ achieves its maximum values at $t=\frac{\pi}{2\alpha}\pm i\frac{\pi}{\alpha},\forall i\in\mathbb{Z}$, while the minimum values occur at $t=0\pm i\frac{\pi}{\alpha},\forall i\in\mathbb{Z}$. Thus, the maxima are reached at points outside the rectangular region for the mapping error, and the minima are inside.

Denoting with $\mathscr{I}$ and $\mathscr{O}$ the inner and outer regions, respectively, the expectation of the function $e_x(t)$ can be approximated as $\mathbb{E}[e_x(t)]=\int e_x(t)p_t(t)\mathrm{d}t\approx\int_{G(\mathscr{I})}e_x(t)p_t(t)\mathrm{d}t+\int_{G(\mathscr{O})}e_x(t)p_t(t)\mathrm{d}t$, where $G(\cdot)$ gives the set of encoded points belonging to a region, and it is an approximation because the regions of both integrals can overlap. Assuming that $\int_{G(\mathscr{I})}p_t(t)\mathrm{d}t\approx\int_{\mathscr{I}}p(\mathbf{x})\mathrm{d}\mathbf{x}$, and similarly for $\mathscr{O}$, if we approximate $e_x(t)$ by its maximum value in the outer region and by its minimum value in the inner region, the expectation term is given by $\mathbb{E}[e_x(t)]\approx\max\{e_x(t)\}\int_{\mathscr{O}}p(\mathbf{x})\mathrm{d}\mathbf{x}+\min\{e_x(t)\}\int_{\mathscr{I}}p(\mathbf{x})\mathrm{d}\mathbf{x}$. According to this expression and the formulation in (37), $u=\int_{\mathscr{O}}p(\mathbf{x})\mathrm{d}\mathbf{x}=1-p_{\text{in}}$ is a reasonable choice, and we checked experimentally that this approach provides good results. On the contrary, $e_y(t)$ achieves its maximum values in the inner region and the maximum ones in the outer region, and in that case we choose $u=\int_{\mathscr{I}}p(\mathbf{x})\mathrm{d}\mathbf{x}=p_{\text{in}}$. The behaviour of the functions $e_x(t)$ and $e_y(t)$ is identical for other scenarios with different mapping parameters.

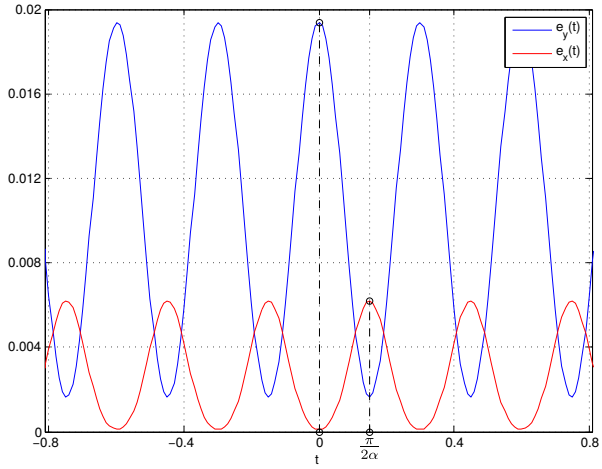

Fig. 4. Example of the error functions $e_{x_i}(t)$ and $e_{y_i}(t)$ for a sine-like mapping with parameters ($\alpha=10;\ \Delta=1.4;\beta=0$).

Taking into account this reasoning, the approximations of the user channel errors are given by

$$\sigma_{N,1}^2\approx\frac{\lambda_1}{2}\left(p_{in}\min\{e_{x_1}\}+(1-p_{in})\max\{e_{x_1}\}\right)+\frac{\lambda_2}{2}(1+\beta)^2\left(p_{in}\max\{e_{y_1}\}+(1-p_{in})\min\{e_{y_1}\}\right)$$
$$=\frac{\lambda_1}{2}\left(p_{in}e_{x_1}(0)+(1-p_{in})e_{x_1}\left(\frac{\pi}{2\alpha}\right)\right)+\frac{\lambda_2}{2}(1+\beta)^2\left(p_{in}e_{y_1}(0)+(1-p_{in})e_{y_1}\left(\frac{\pi}{2\alpha}\right)\right)$$

$$\sigma_{N,2}^2\approx\frac{\lambda_1}{2}\left(p_{in}\min\{e_{x_2}\}+(1-p_{in})\max\{e_{x_2}\}\right)+\frac{\lambda_2}{2}(1-\beta)^2\left(p_{in}\max\{e_{y_2}\}+(1-p_{in})\min\{e_{y_2}\}\right)$$
$$=\frac{\lambda_1}{2}\left(p_{in}e_{x_2}(0)+(1-p_{in})e_{x_2}\left(\frac{\pi}{2\alpha}\right)\right)+\frac{\lambda_2}{2}(1-\beta)^2\left(p_{in}e_{y_2}(0)+(1-p_{in})e_{y_2}\left(\frac{\pi}{2\alpha}\right)\right),$$

with

$$e_{x_i}(0) = \sigma_{n_i}^2\left(1-2\exp\left(-2\alpha^2\sigma_{n_i}^2\right)\right) + \frac{1}{4\alpha^2}\left(\exp\left(-\frac{1}{2}\exp(-8\alpha^2\sigma_{n_i}^2)+\frac{1}{2}\right)\right)$$

$$e_{x_i}\left(\frac{\pi}{2\alpha}\right) = \sigma_{n_i}^2\left(1+2\exp\left(-2\alpha^2\sigma_{n_i}^2\right)\right) + \frac{1}{4\alpha^2}\left(\exp\left(-\frac{1}{2}\exp(-8\alpha^2\sigma_{n_i}^2)+\frac{1}{2}\right)\right)$$

$$e_{y_i}(0) = \Delta^2\left(-\frac{1}{2}\exp(-2\alpha^2\sigma_{n_i}^2)+\frac{1}{2}\right)$$

$$e_{y_i}\left(\frac{\pi}{2\alpha}\right) = \Delta^2\left(-2\exp\left(-\frac{\alpha^2\sigma_{n_i}^2}{2}\right)+\frac{1}{2}\exp(-2\alpha^2\sigma_{n_i}^2)+\frac{3}{2}\right).$$

Like in the mapping error, the same noise error is obtained for both users if $\beta = 0$. Otherwise, these errors are no longer equal and the difference depends on the specific value of the β parameter.

3) Residual Term: The last contribution on the overall user distortions $\xi_i^{\sin}$ is the term

$$\gamma_i = 2\mathbb{E}\left[(x_i-\bar{x}_i)(\hat{x}_i-\bar{x}_i)\right].$$

When computing the expectation, the term $(x_i-\bar{x}_i)$ only depends on the source space, while the term $(\hat{x}_i-\bar{x}_i)$ only depends on the noise. Hence, the expectation in the above expression can be computed as $\gamma_i = 2\mathbb{E}[\hat{x}_i-\bar{x}_i]\mathbb{E}[x_i-\bar{x}_i]$.

Assuming the minimum distance encoder is used, each point of the source space is orthogonally projected on the parametric curve, and the vectors corresponding to the mapping errors $(x_i-\bar{x}_i)$ can be represented by a normalized orthogonal vector to the tangent of the curve at each point (see Figure 1). In particular, we consider

$$\mathbf{d}(t) = \left[-\frac{\mathrm{d}c_y(t)}{\mathrm{d}t}, \frac{\mathrm{d}c_x(t)}{\mathrm{d}t}\right]^T = [d_1(t)\ d_2(t)]^T, \qquad (38)$$

where

$$d_1(t) = \sqrt{\frac{\lambda_1}{2}}(1-\cos(2\alpha t)) + \sqrt{\frac{\lambda_2}{2}}(1+\beta)\Delta\alpha\cos(\alpha t)$$

$$d_2(t) = \sqrt{\frac{\lambda_1}{2}}(1-\cos(2\alpha t)) + \sqrt{\frac{\lambda_2}{2}}(1-\beta)\Delta\alpha\cos(\alpha t).$$

The normalized version of these orthogonal vectors is $\tilde{\mathbf{d}}(t) = \mathbf{d}(t)/\|\mathbf{d}(t)\|^2$. This error is a consequence of the non-orthogonality of the vectors for the mapping error and the noise error and, therefore, it is only significant for source points outside the rectangle. Hence, the first component of the residual term can be approximated by the normalized orthogonal vectors $\tilde{\mathbf{d}}(t)$ weighted by the mean mapping error corresponding to the points outside the rectangle, i.e., $\sqrt{\frac{\lambda_2}{2}e_{\text{out}}}\tilde{\mathbf{d}}(t)$.

The term corresponding to the noise effect, i.e. $(x_i-\bar{x}_i)$, can be calculated for each user following a reasoning similar to that of the previous section. In this case, we define

$$B_1(t) = \mathbb{E}[x_1-\bar{x}_1] = \int p_{n_1}(n)(c_x(t)-c_x(t+n))\mathrm{d}n \qquad (39)$$

$$B_2(t) = \mathbb{E}[x_2-\bar{x}_2] = \int p_{n_2}(n)(c_y(t)-c_y(t+n))\mathrm{d}n. \qquad (40)$$

Replacing $c_x(t)$ and $c_y(t)$ by their corresponding expressions given by (33) and (34), respectively, and solving the resulting integrals, we obtain

$$B_1(t) = \sqrt{\frac{\lambda_1}{2}}\frac{1}{2\alpha}\sin(2\alpha t)(\exp(-2\sigma_{n_1}^2\alpha^2)-1) + \sqrt{\frac{\lambda_2}{2}}(1+\beta)\Delta\sin(\alpha t)\left(\exp\left(-\frac{\sigma_{n_1}^2\alpha^2}{2}\right)-1\right)$$

$$B_2(t) = \sqrt{\frac{\lambda_1}{2}}\frac{1}{2\alpha}\sin(2\alpha t)(\exp(-2\sigma_{n_2}^2\alpha^2)-1) - \sqrt{\frac{\lambda_2}{2}}(1-\beta)\Delta\sin(\alpha t)\left(\exp\left(-\frac{\sigma_{n_2}^2\alpha^2}{2}\right)-1\right).$$

The intermediate steps to obtain the above result from (39) and (40) are detailed in Appendix D. The residual terms at the point t are hence given by

$$\gamma_i(t) \approx 2\sqrt{\frac{\lambda_2}{2}e_{\text{out}}}\ [\tilde{\mathbf{d}}(t)]_i B_i(t) \qquad (41)$$

Like in the case of the noise error, the resulting expressions explicitly depend on t. To circumvent this problem we follow a similar strategy, i.e. we approach the expectation of the above expression by using a convex combination of the extreme points. Recall that the impact of this term is only significant for the source points outside the rectangle. On one hand, the minimum values of the residual term in the outer region are practically zero, and they correspond to the points on the intersection between the top and bottom edges of the rectangle and the mapping curve. On the other, the maximum values are around the top and bottom of the curve and correspond to less likely points of the source space. Hence, it is reasonable to conclude that the weight of the points with lower residual error must be larger than the points with larger error. For this reason, we propose $u = 1/4$ as convex combination factor. In this case, the residual term is approximated as

$$\gamma_i \approx \frac{1}{4}\max_t\left[2\sqrt{\frac{\lambda_2}{2}e_{\text{out}}}\ [\tilde{\mathbf{d}}(t)]_i B_i(t)\right], \qquad (42)$$

since the minimum value of (41) on the region of interest is assumed to be 0. Factors around this value have been shown to provide good approximations of the residual error.

C. Algorithm for the Optimization of Sine-Like Mappings

In the previous sections, we derived an expression for the overall distortion at each BC user when a sine-like mapping is used to encode the source symbols. This expression depends on the three mapping parameters (Δ, α and β) and provides approximations of the user distortions for any combination of such parameters. Our objective now is to find the combination of values that satisfy the requirements in terms of individual distortions. As commented in Section II, we consider the balancing of the user distortions to guarantee the feasibility of the resulting optimization problems. Let ε_1 and ε_2 be the initial distortion targets for the two users. Then, the optimal values of the mapping parameters can be obtained as the solution of the following optimization problem

$$\min_{\alpha,\Delta,\beta}\ b \qquad s.t.\ \ \xi_i^{\sin}(\alpha,\Delta,\beta) - b\varepsilon_i \le 0; \qquad (43)$$

where

$$\xi_i^{\sin}(\alpha,\Delta,\beta) = \sigma_{A,i}^2 + \sigma_{N,i}^2 - \gamma_i \quad i = 1,2. \tag{44}$$

Since (43) is not convex, because the error equations are not convex, we propose an algorithm based on an exhaustive search on the β space so that the optimal α and Δ values for each considered β are determined, and the combination with lowest distortion is chosen. Thereby, the algorithm comprises two main stages: 1) given β, the bisection method is employed to find the minimum b that satisfies the problem constraints, and the corresponding α and Δ are obtained; 2) the previous step is carried out for a collection of β values in the interval $[-1,1]$, and the combination that provides the lowest distortion is finally chosen.

This algorithm allows, with the help of the MSE approximation of the sine-like mappings, to lower the computational complexity of the search of the optimal parameters. The use of the approximation derived in the previous section avoids to compute the MSEs by Monte Carlo techniques which are computationally unaffordable for the large number of symbols required in the simulations to obtain proper approximations of the user distortions.

V. Results

In this section, the results of several computer experiments are presented to illustrate the performance of the proposed analog JSCC scheme for Gaussian BC scenarios with individual distortion targets. Source symbols are assumed to follow a bivariate Gaussian distribution with zero mean and covariance matrix $\mathbf{C_x} = [1\ \rho;\rho\ \ 1]$, where ρ determines the correlation between symbols. Each pair of source symbols is encoded using an analog mapping and sent over the Gaussian BC. The transmitted symbols are normalized to ensure the transmit power is equal to 1. For convenience, we focus on the symmetric case where the noise variance for both users is the same, σ_n^2. Hence, the SNR is $\eta = 1/\sigma_n^2$. At each receiver, the source symbols are decoded using an appropriate strategy, and the individual distortions are computed from the MSE between the source and the estimated symbols as $\xi_i = \mathbb{E}\left[|\hat{x}_i - x_i|^2\right], \quad i = 1,2$. The performance of the analog JSCC system is measured in terms of the Signal-to-Distortion Ratio (SDR), which is defined for each receiver as

$$\mathrm{SDR}_i[\mathrm{dB}] = 10\log_{10}(1/\xi_i). \tag{45}$$

As introduced in Section II-A, three distortion regions can be distinguished when sending a bivariate Gaussian. These regions are delimited by the two SNR thresholds presented in (8). The optimal strategy in the first region consists of sending the symbols of one user only. In the second region, it is known that the uncoded scheme with the MMSE decoder is able to achieve the OPTA as long as it is properly optimized. Hence, it is sensible to restrict the optimization and use of sine-like mappings to the third SNR region given by

$$\eta \geq v(\rho,k) + \sqrt{v(\rho,k)\,(v(\rho,k)-1)}, \tag{46}$$

with $v(\rho,k) = \frac{k^2+2k\rho+1}{2k(1-\rho^2)} - 1$ and k the ratio between the distortion targets for the two users.

TABLE I
Optimal parameters for the sine-like mapping with $\rho = 0.9$ and equal user targets $k = 1$.

	Parameter α				Parameter Δ			
SNR	15	20	25	30	15	20	25	30
LS Fitting	5.11	6.9	8.2	10.39	0.16	0.93	1.2	1.44
Searching Alg.	33.5	7.0	8.7	10.1	0.34	0.98	1.12	1.28

In the first experiment, the algorithm for the optimization of the sine-like mappings is tested, and the accuracy of the distortion approximation obtained in Section IV-B for these mappings is also assessed. Table I compares the values obtained for the parameters of the sine-like mapping with two different optimization approaches: 1) least square fitting of the obtained non-parametric mappings, and 2) the searching algorithm explained in Section IV-C using the distortion approximations. The correlation factor for the source symbols is $\rho = 0.9$ and the same distortion target is assumed for the two users, i.e. $k = 1$. Therefore, the region of interest is given by the SNRs such that $\eta \geq 12.6$ dB. As observed, both optimization strategies provide quite similar parameters for $\eta \geq 20$ dB and, in fact, the analog scheme using the mapping parameters of either strategy achieves an almost identical distortion. For $\eta = 15$ dB, the resulting mappings resemble a linear encoding since Δ is near zero. Different values for α are obtained depending on the optimization approach, but in this case that parameter is less significant and similar performance is achieved.

Table II shows the optimal parameters, obtained with the proposed algorithm, for different ratios of the user targets, in particular, $k = 1, k = 1.5, k = 2$ and $k = 4$, and their corresponding SNR thresholds. As observed, the value of β increases for all SNRs as the distortion ratio k is larger, i.e. as the difference between the user distortions grows. Regarding the other parameters, the optimal α and Δ values are also larger as k increases. Thus, the analog scheme aims to satisfy the balancing of the user distortions by changing not only the slope of the mapping but also the amplitude and the frequency of the sine function. Figure 5 shows the resulting sine-like mappings for $k = 1$ (left side) and $k = 4$ (right side), with the optimal parameters obtained for SNR $= 25$ dB and $\rho = 0.9$. As observed, for $k = 4$, the mapping is skewed to the right with respect to the mappping for $k = 1$. When the mapping is transformed this way, the central part of the sine tends to be more vertical and, as a consequence, the decoding error for the first user will be lower. This is the reason why β increases with k, since more unbalanced targets demand more protection to one user, and β helps by skewing the mapping.

We next compare the distortion determined analytically in Section IV and the actual distortion obtained in simulation for $k = 2$ and the optimal sine-like mapping parameters. Figure 6 shows the two SDR curves for the two BC users in the considered SNR region. The optimal performance bounds for this scenario are calculated according to (8) and (9), and plotted in the figure for comparison. As observed, the expression derived to approximate the distortion of sine-like

TABLE II
OPTIMAL PARAMETERS FOR THE SINE-LIKE MAPPING WITH $\rho = 0.9$ AND DIFFERENT k VALUES.

		Parameter α				Parameter Δ				Parameter β			
	SNR	15	20	25	30	15	20	25	30	15	20	25	30
$k=1$	12.55	33.5	7.0	8.7	10.1	0.34	0.98	1.12	1.28	0	0	0	0
$k=1.5$	12.78	34.0	7.81	9.66	11.41	0.4	1.08	1.21	1.4	0.56	0.46	0.41	0.4
$k=2$	13.15	34.0	8.61	10.08	11.68	0.51	1.09	1.26	1.45	0.76	0.61	0.55	0.56
$k=4$	14.75	42.6	10.82	12.23	12.65	0.88	1.21	1.33	1.57	0.82	0.74	0.69	0.78

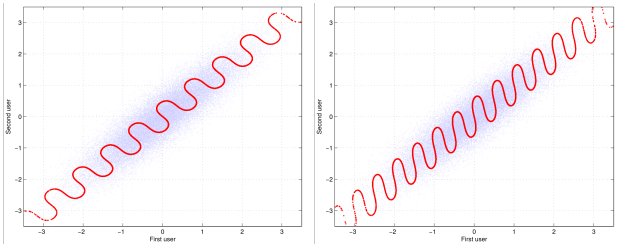

Fig. 5. Sine-like mappings with the obtained optimal parameters for $k = 1$ and $k = 4$ with $\rho = 0.9$ and SNR = 25 dB.

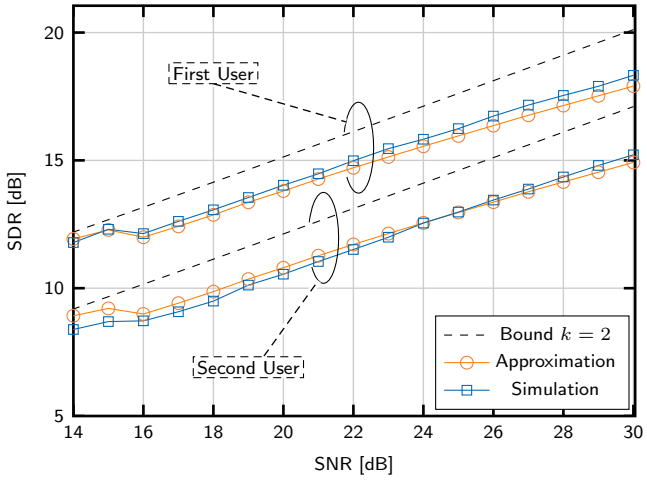

Fig. 6. Comparison between the user distortions obtained with the approximation and by simulation for $k = 2$ with $\rho = 0.9$.

mappings provides accurate results since the difference with respect to the actual distortion in simulation is less than 0.3 dB for the whole SNR range. In addition, both curves approach the corresponding performance bounds and, therefore, we can conclude that the approximation function is able to obtain good estimates of the optimal values for the mapping parameters.

In the second experiment, the performance of optimized sine-like mappings with different strategies at the encoding and decoding steps is evaluated for the case of symmetric distortions and $\rho = 0.9$. In particular, we evaluate five possible configurations: 1) Minimum Distance (MD) mapping and ML decoder, 2) MD mapping and the two stage receiver (linear MMSE+ML), 3) Expected Distortion (ED) mapping + ML decoder, 4) MD mapping + MMSE decoder and 5) ED mapping + MMSE decoder. The performance curves obtained are shown in Figure 7. The SDR curve corresponding to the analog scheme with non-parametric mappings and the appropriate performance bound are also included in the figure. As observed, the differences on the performance for all the

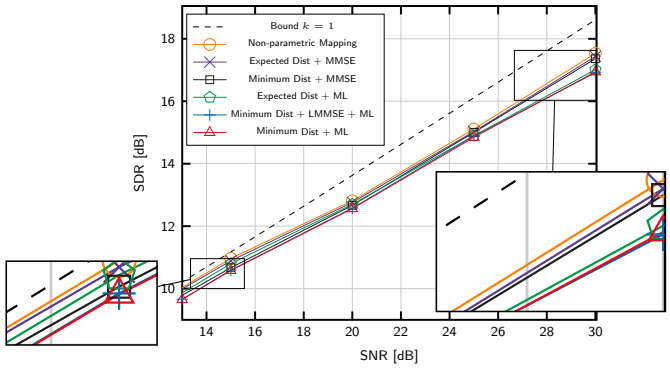

Fig. 7. Performance of the sine-like mapping with different methods for the encoding and decoding operation with a correlation factor $\rho = 0.9$ and symmetric distortions ($k = 1$).

configurations are quite small for all SNR values. On the one hand, the addition of the linear MMSE filter does not contribute to increase the SDR for the range of considered SNRs. On the other, the ED method provides a slight gain for medium SNRs (about 0.3 dB in SNR = 15 dB), but at the expense of increasing the encoding complexity. Finally, the use of the optimal MMSE decoder reduces the gap with respect to the non-parametric one in the high SNR region, also at the expense of increasing the complexity significantly. Notice that the parametric sine-like mappings are able to approach the performance of the non-parametric ones with much less complexity.

Figure 8 compares the performance of parametric sine-like mappings to that of other parametric analog JSCC mappings. The first one is the uncoded mapping described in Section III-A using the optimization approach explained in Section IV-A. The second is a variant of the Scalar Quantizer Linear Coder (SQLC) [29] referred to as alternating sign SQLC and was proposed in [27] for bivariate Gaussian sources and BCs. Finally, we consider the Archimedean spiral [14], [15], traditionally employed for the 2:1 compression of independent sources. For low and medium SNRs, the best performance corresponds to the uncoded scheme, achieving even the performance bound in this region. However, it saturates for high SNRs where the best results are provided by the parametric sine-like mapping. These results confirm the optimality of the uncoded scheme in the two first regions and the suitability of sine-like mappings for the last one.

In the next experiment, we considered scenarios with different distortion targets and balancing of the individual distortions. Figure 9 shows the user SDRs obtained for $k = 2$ when a bivariate Gaussian source with $\rho = 0.8$ is transmitted using an optimized analog JSCC system. This means that the system

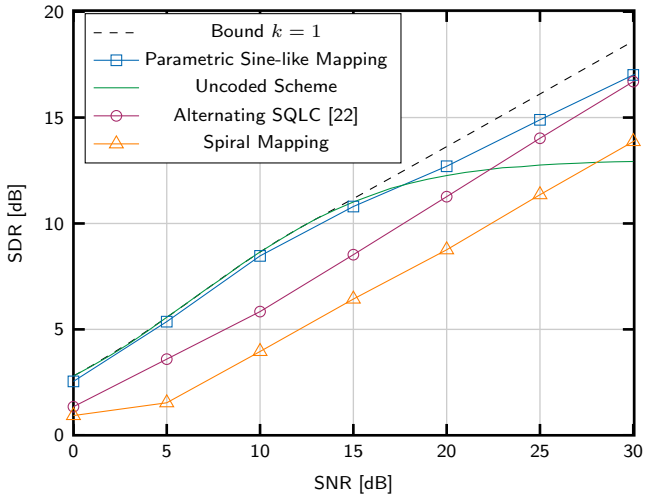

Fig. 8. Performance comparison between different analog JSCC mappings for $\rho = 0.9$ and symmetric distortion targets.

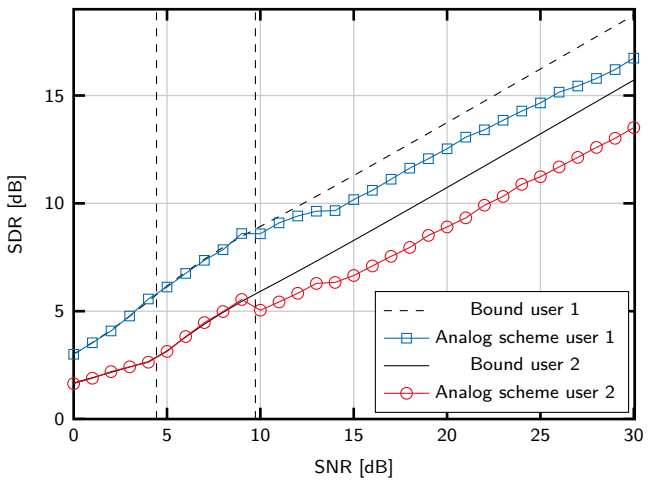

Fig. 9. Performance of the optimized analog JSCC scheme and the corresponding performance bounds for a correlation factor $\rho = 0.8$ and a balancing ratio $k = 2$. Dashed vertical lines mark the SNR values where the encoder changes.

uses the best mapping at each SNR region. The SNR values where the encoder switches are marked with dashed vertical lines. In the lowest SNR region, the symbols of one user are directly transmitted over the channel. In the second one, the uncoded scheme with the optimal parameters is employed, whereas in the highest SNR region the optimized parametric sine-like mapping is selected to encode the source data. The optimal performance bound for a balancing factor $k = 2$ is also plotted in the figure. As observed, the performance of the proposed scheme perfectly matches that of the theoretical bounds for $\eta < 9.7$ dB, which corresponds to the two first distortion regions where the uncoded scheme is the optimal strategy. For larger SNRs, the sine-like mapping provides a near optimal performance, although the gap with respect to the theoretical bounds is between 1 and 1.8 dB. The simulation results also confirm that the analog system properly balances the user distortions according to the k value, since the gap between the SDR curves for the two users is about 3 dB. In the first region ($\eta < 4.6$ dB) this gap is smaller than 3 dB because the balancing is only possible by penalizing the second user, and its actual performance is directly determined by the error covariance of the linear MMSE estimator.

Figure 10 shows the same SDR curves and performance bounds when $\rho = 0.95$. The results are similar to those of the previous scenario, although we can remark two slight differences. One is the SDR gain obtained for both users in medium and large SNRs since the analog scheme is able to exploit the larger source correlation. In this case, the gap between the SDR curves and the theoretical bounds remains about 1 dB in the third region. The other is the SNR threshold beyond which the sine-like mapping is employed to encode the user symbols, which is now much higher (16.4 dB). Like in the previous case, the gap between the SDR curves is about 3 dB in the medium and high SNR region and, therefore, the analog scheme satisfies the balanced distortion targets.

Finally, we test the proposed optimization method for different ratios between the user targets. In particular, the performance of the parametric sine-like mapping with optimal

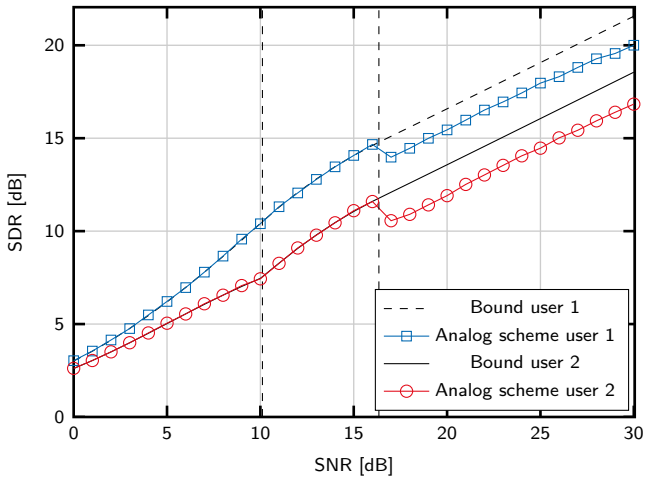

Fig. 10. Performance of the analog JSCC scheme and the corresponding performance bounds for $\rho = 0.95$ and a balancing ratio $k = 2$.

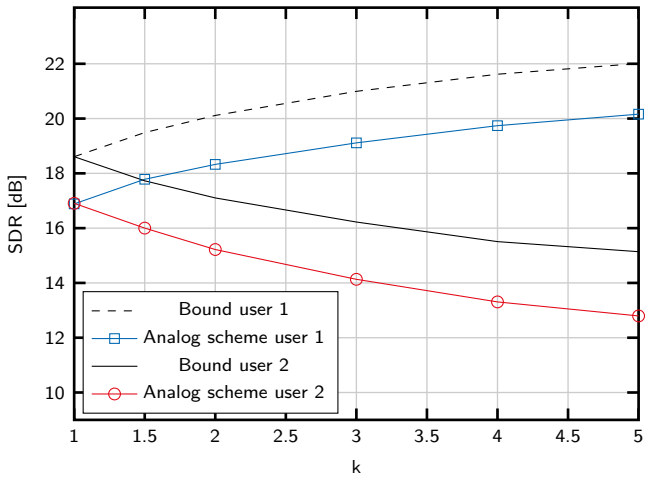

Fig. 11. SDR curves and the performance bounds for the two BC users considering several balancing factors for SNR = 30 dB and $\rho = 0.9$.

parameters is shown in Figure 11 for $\rho = 0.9$ and $\eta = 30$ dB and different values of k. As expected, the gap between the performance curves of the BC users increases with k. In addition, the gap with respect to the bounds remains constant at about 2 dB for the considered k values. This behaviour confirms that the analog JSCC system is able to satisfy different quality of service requirements, even when the user targets are significantly different.

VI. Conclusion

We have addressed the analog transmission of bivariate Gaussian symbols over BCs using analog JSCC mappings. The analog scheme has been designed to satisfy individual quality of service requirements, and the balancing of the user distortions has also been considered to ensure the feasibility of the optimization problems. In particular, two types of analog parametric mappings have been optimized for different SNR regions supporting the distortion balancing on BC communications. The resulting analog JSCC system has been shown to provide near optimal performance with high transmission rate, low complexity and negligible delay thanks to the use of parametric mappings. This scheme is designed for the case of two receivers, where it is affordable to obtain closed-form approximations for the mapping distortion. A suboptimal strategy for a larger number of users consists in combining several 2:1 encoders in parallel, but this strategy does not exploit the source correlation completely. The proposed scheme can be easily adapted to fading BCs by using the equivalent noise variances after the filtering stage in the distortion expressions.

VII. Acknowledgements

This work has been funded in part by NSF Award CCF-1618653, ONRG of United States (N62909-15-1-2014), the Xunta de Galicia (ED431C 2016-045, ED431G/01), the Agencia Estatal de Investigación of Spain (TEC2013-47141-C4-1-R, TEC2016-75067-C4-1-R) and ERDF funds of the EU (AEI/FEDER, UE).

Appendix A
Height estimate for the Approximation Mapping

The parameter $\bar{\Delta}$ is obtained from the unprojected mapping. First, we look for the point $\bar{t}$ where the derivative of the mapping matches some threshold U

$$\frac{\mathrm{d}s_x(\bar{t})}{\mathrm{d}s_y(\bar{t})} = \frac{1-\cos(2\alpha\bar{t})}{\Delta\alpha\cos(\alpha\bar{t})} = U, \tag{47}$$

Using $\cos(2x) = 2\cos^2(x) - 1$, the point $\bar{t}$ can be found by solving

$$2 - 2\cos^2(\alpha\bar{t}) - U\Delta\alpha\cos(\alpha\bar{t}) = 0. \tag{48}$$

Solving for $y = \cos(\alpha\bar{t})$, we obtain $y = \frac{U\Delta\alpha \pm \sqrt{(U\Delta\alpha)^2+16}}{-4}$ and, therefore, $\bar{t} = \frac{1}{\alpha}\arccos(y)$. Finally, $\bar{\Delta}$ is found by determining the y-coordinate of the mapping at $\bar{t}$, i.e.

$$\bar{\Delta} = \Delta\sin(\alpha\bar{t}) = \Delta\sin(\arccos(y)) \tag{49}$$

Given that $\sin(\arccos(y)) = \sqrt{1-y^2}$ and operating on the resulting expression, we arrive at

$$\bar{\Delta} = \frac{U\alpha\Delta^2}{4}\sqrt{-2+2\sqrt{1+\left(\frac{4}{U\alpha\Delta}\right)^2}} \tag{50}$$

Appendix B
Mapping error in the outer region

From the unprojected mapping, the error in the outer region can be approximated by the mean squared error between each point in that region and the $\bar{\Delta}$ line

$$e_{\text{quad}} = \frac{1}{2\pi}\int_{-\infty}^{-\bar{\Delta}}\int_{-\infty}^{0} |x_2+\bar{\Delta}|^2 \exp\left(-\frac{x_1^2+x_2^2}{2}\right)\mathrm{d}x_1\,\mathrm{d}x_2, \tag{51}$$

$$\begin{aligned} e_{\text{quad}} &= \frac{1}{2\pi}\int_{-\infty}^{0}\exp\left(-\frac{x_1^2}{2}\right)\mathrm{d}x_1 \int_{-\infty}^{-\bar{\Delta}}(x_2^2+\bar{\Delta}^2+2x_2\bar{\Delta})\exp\left(-\frac{x_2^2}{2}\right)\mathrm{d}x_2 \\ &= \frac{1}{2\sqrt{2\pi}}\int_{-\infty}^{-\bar{\Delta}}(x_2^2+\bar{\Delta}^2+2\bar{\Delta}x_2)\exp\left(-\frac{x_2^2}{2}\right)\mathrm{d}x_2, \end{aligned} \tag{52}$$

Using the following identities

$$\begin{aligned} &\frac{1}{\sqrt{2\pi}}\int_{-\infty}^{t} x^2\exp\left(-\frac{x^2}{2}\right)\mathrm{d}x = \\ &\qquad \frac{1}{2}\left(1+\operatorname{erf}\left(-\frac{t}{\sqrt{2}}\right)\right) + \frac{t}{\sqrt{2\pi}}\exp\left(-\frac{t^2}{2}\right), \end{aligned} \tag{53}$$

$$\frac{1}{\sqrt{2\pi}}\int_{-\infty}^{t}\exp\left(-\frac{x^2}{2}\right)\mathrm{d}x = \frac{1}{2}\left(1+\operatorname{erf}\left(-\frac{t}{\sqrt{2}}\right)\right), \tag{54}$$

$$\frac{1}{\sqrt{2\pi}}\int_{-\infty}^{t} x\exp\left(-\frac{x^2}{2}\right)\mathrm{d}x = \frac{1}{\sqrt{2\pi}}\exp\left(-\frac{t^2}{2}\right), \tag{55}$$

we obtain

$$\begin{aligned} e_{\text{quad}} = \frac{1}{2}\Bigg[&\frac{1}{2}\left(1+\operatorname{erf}\left(-\frac{\bar{\Delta}}{\sqrt{2}}\right)\right) + \frac{\bar{\Delta}}{\sqrt{2\pi}}\exp\left(-\frac{\bar{\Delta}^2}{2}\right) \\ &+ \frac{\bar{\Delta}}{2}\left(1+\operatorname{erf}\left(-\frac{\bar{\Delta}}{\sqrt{2}}\right)\right) - \frac{2\bar{\Delta}}{\sqrt{2\pi}}\exp\left(-\frac{\bar{\Delta}^2}{2}\right)\Bigg]. \end{aligned} \tag{56}$$

Sorting the common terms, the above expression simplifies to

$$e_{\text{quad}} = \frac{1}{2}\left(\frac{1}{2}(1+\bar{\Delta})\left(1+\operatorname{erf}\left(-\frac{\bar{\Delta}}{\sqrt{2}}\right)\right) - \frac{\bar{\Delta}}{\sqrt{2\pi}}\exp\left(-\frac{\bar{\Delta}^2}{2}\right)\right) \tag{57}$$

Finally, since $e_{\text{out}} = 4e_{\text{quad}}$, the outside error is given by

$$e_{\text{out}} = (1+\bar{\Delta})\left(1+\operatorname{erf}\left(-\frac{\bar{\Delta}}{\sqrt{2}}\right)\right) - \frac{2\bar{\Delta}}{\sqrt{2\pi}}\exp\left(-\frac{\bar{\Delta}^2}{2}\right) \tag{58}$$

Appendix C
Computation of the error components in the channel error

We start from the definition of $e_{x_i}(t)$ and $e_{y_i}(t)$ given by

$$e_{x_i}(t) = \int p_{n_i}(n)|s_x(t) - s_x(t+n)|^2\mathrm{d}n \tag{59}$$

$$e_{y_i}(t) = \int p_{n_i}(n)|s_y(t) - s_y(t+n)|^2\mathrm{d}n \tag{60}$$

Using the identities

$$\int p_{n_i}(n)\sin(\alpha(t+n))\mathrm{d}n = \sin(\alpha t)\exp\left(-\frac{\alpha^2\sigma_{n_i}^2}{2}\right), \quad (61)$$

$$\int p_{n_i}(n)\sin^2(\alpha(t+n))\mathrm{d}n = \frac{1}{2} - \frac{1}{2}\cos(2\alpha t)\exp(-2\alpha^2\sigma_{n_i}^2) \quad (62)$$

it can be shown that

$$a_\alpha(t) = \int p_{n_i}(n)|\sin(\alpha t) - \sin(\alpha(t+n))|^2\mathrm{d}n = 1 - \exp\left(-\frac{\alpha^2\sigma_{n_i}^2}{2}\right) + \cos(2\alpha t)\left(\exp\left(\frac{-\alpha^2\sigma_{n_i}^2}{2}\right) - \frac{1}{2}\exp(-2\alpha^2\sigma_{n_i}^2) - \frac{1}{2}\right).$$

Using this identity, it is straightforward to get an expression for (60), where $s_y(t) = \Delta\sin(\alpha t)$

$$e_{y_i}(t) = \int p_{n_i}(n)|\Delta\sin(\alpha t) - \Delta\sin(\alpha(t+n))|^2\mathrm{d}n = \Delta^2 a_\alpha(t) \quad (63)$$

Now, for $s_x(t) = t - \frac{1}{2\alpha}\sin(2\alpha t)$ we have

$$\begin{aligned} e_{x_i}(t) = & \int p_{n_i}(n)\left|t - \frac{1}{2\alpha}\sin(2\alpha t) - (t+n - \frac{1}{2\alpha}\sin(2\alpha(t+n)))\right|^2 \mathrm{d}n \\ = & \int n^2 p_{n_i}(n)\mathrm{d}n + \frac{1}{4\alpha^2}\int p_{n_i}(n)|sin(2\alpha t) - \sin(2\alpha(t+n))|^2\mathrm{d}n \\ & - \frac{1}{\alpha}\int p_{n_i}(n)n(\sin(2\alpha t) - \sin(2\alpha(t+n))\mathrm{d}n \\ = & \sigma_{n_i}^2 + \frac{1}{4\alpha^2}a_{2\alpha}(t) - \frac{1}{\alpha}\int p_{n_i}(n)n\sin(2\alpha(t+n))\,\mathrm{d}n \end{aligned} \quad (64)$$

Finally, using the identity

$$\int n p_{n_i}(n)\sin(\alpha(t+n))\mathrm{d}n = \alpha\sigma_{n_i}^2\cos(\alpha t)\exp\left(-\frac{\alpha^2\sigma_{n_i}^2}{2}\right), \quad (65)$$

we get

$$e_{x_i}(t) = \sigma_{n_i}^2 + \frac{1}{4\alpha^2}a_{2\alpha}(t) - 2\sigma_{n_i}^2\cos(2\alpha t)\exp(-2\alpha^2\sigma_{n_i}^2).$$

Replacing $a_{2\alpha}(t)$ by its expression and rearranging terms, we finally obtain

$$\begin{aligned} e_{x_i}(t) = & \sigma_{n_i}^2\left(1 - 2\cos(2\alpha t)\exp\left(-2\alpha^2\sigma_{n_i}^2\right)\right) \\ & + \frac{1}{4\alpha^2}(1 - \exp(-2\alpha^2\sigma_{n_i}^2)) \\ & + \frac{1}{4\alpha^2}\cos(4\alpha t)\left(\exp\left(-2\alpha^2\sigma_{n_i}^2\right) - \frac{1}{2}\exp(-8\alpha^2\sigma_{n_i}^2) - \frac{1}{2}\right). \end{aligned} \quad (66)$$

APPENDIX D
RESIDUAL ERROR

Starting from

$$\begin{aligned} B_1(t) &= \int p_{n_1}(n)(c_x(t) - c_x(t+n))\mathrm{d}n \\ &= c_x(t) - \int p_{n_1}(n)c_x(t+n)\mathrm{d}n \\ B_2(t) &= \int p_{n_2}(n)(c_y(t) - c_y(t+n))\mathrm{d}n \\ &= c_y(t) - \int p_{n_2}(n)c_y(t+n)\mathrm{d}n, \end{aligned}$$

and using the expressions for $c_x(t)$ and $c_y(t)$ given in (33) and (34), we obtain

$$\begin{aligned} B_1(t) = & \left(\sqrt{\frac{\lambda_1}{2}}s_x(t+n) + \sqrt{\frac{\lambda_2}{2}}(1+\beta)s_y(t+n)\right) \\ & - \int p_{n_1}(n)\left(\sqrt{\frac{\lambda_1}{2}}s_x(t+n) + \sqrt{\frac{\lambda_2}{2}}(1+\beta)s_y(t+n)\right)\mathrm{d}n \\ B_2(t) = & \left(\sqrt{\frac{\lambda_1}{2}}s_x(t+n) - \sqrt{\frac{\lambda_2}{2}}(1-\beta)s_y(t+n)\right) \\ & - \int p_{n_2}(n)\left(\sqrt{\frac{\lambda_1}{2}}s_x(t+n) - \sqrt{\frac{\lambda_2}{2}}(1-\beta)s_y(t+n)\right)\mathrm{d}n \end{aligned}$$

These integrals can be solved using the property in (61) as follows

$$\begin{aligned} \int p_{n_1}(n)s_x(t+n)\mathrm{d}n &= \int p_{n_1}(n)\left(t - \frac{1}{2\alpha}\sin(2\alpha(t+n))\right)\mathrm{d}n \\ &= t - \frac{1}{2\alpha}\sin(2\alpha t)\exp(-2\alpha^2\sigma_{n_1}^2) \\ \int p_{n_2}(n)s_y(t+n)\mathrm{d}n &= \int p_{n_2}(n)\Delta\sin(\alpha(t+n))\mathrm{d}n \\ &= \Delta\sin(\alpha t)\exp\left(-\frac{\alpha^2\sigma_{n_2}^2}{2}\right) \end{aligned}$$

Finally, using these identities we obtain

$$\begin{aligned} B_1(t) = & \sqrt{\frac{\lambda_1}{2}}\frac{1}{2\alpha}\sin(2\alpha t)(\exp(-2\sigma_{n_1}^2\alpha^2) - 1) \\ & + \sqrt{\frac{\lambda_2}{2}}(1+\beta)\Delta\sin(\alpha t)\left(\exp\left(-\frac{\sigma_{n_1}^2\alpha^2}{2}\right) - 1\right) \\ B_2(t) = & \sqrt{\frac{\lambda_1}{2}}\frac{1}{2\alpha}\sin(2\alpha t)(\exp(-2\sigma_{n_2}^2\alpha^2) - 1) \\ & - \sqrt{\frac{\lambda_2}{2}}(1-\beta)\Delta\sin(\alpha t)\left(\exp\left(-\frac{\sigma_{n_2}^2\alpha^2}{2}\right) - 1\right). \end{aligned}$$

REFERENCES

[1] C. E. Shannon, "A mathematical theory of communication," *The Bell System Technical Journal*, vol. 7, pp. 379–423, 1948.

[2] D. Tse and P. Viswanath, *Fundamentals of Wireless Communication*. Cambridge University Press, 2005.

[3] M. Costa, "Writing on dirty paper," *IEEE Trans. Inform. Theory*, vol. 29, pp. 439–441, May 1983.

[4] C. Tian, J. Chen, S. Diggavi, and S. Shamai, "Optimality and approximate optimality of source-channel separation in networks," *IEEE Trans. Inform. Theory*, vol. 60, no. 2, pp. 904–918, Feb 2014.

[5] D. Gunduz, E. Erkip, A. Goldsmith, and V. Poor, "Source and channel coding for correlated sources over multiuser channels," *IEEE Trans. Inform. Theory*, vol. 55, no. 9, pp. 3927–3944, Sep 2009.

[6] S. Choi and S. S. Pradhan, "A graph-based framework for transmission of correlated sources over broadcast channels," *IEEE Trans. Inform. Theory*, vol. 54, no. 7, pp. 2841–2856, July 2008.

[7] A. A. Saleh, F. Alajaji, and W. Y. Chan, "Source-interference recovery over broadcast channels: Asymptotic bounds and analog codes," *IEEE Trans. Commun.*, vol. 64, no. 8, pp. 3406–3418, Aug 2016.

[8] H. Behroozi, F. Alajaji, and T. Linder, "On the performance of hybrid digital-analog coding for broadcasting correlated gaussian sources," *IEEE Trans. Commun.*, vol. 59, no. 12, pp. 3335–3342, December 2011.

[9] E. Koken and E. Tuncel, "Joint source-channel coding for broadcasting correlated sources," in *2016 IEEE International Symposium on Information Theory (ISIT)*, July 2016, pp. 1844–1848.

[10] T. P. Coleman, E. Martinian, and E. Ordentlich, "Joint source-channel coding for transmitting correlated sources over broadcast networks," *IEEE Trans. Inform. Theory*, vol. 55, no. 8, pp. 3864–3868, Aug 2009.

[11] C. E. Shannon, "Communication in the presence of noise," *Proceedings of the IRE*, vol. 37, no. 1, pp. 20–21, 1949.

[12] V. Kotel'nikov, *The theory of optimum noise immunity*. New York: McGraw-Hill, 1959.

[13] S. Y. Chung, "On the construction of some capacity-approaching coding schemes," *Ph.D. Dissertation, Dept. EECS, MIT*, 2000.

[14] T. A. Ramstad, "Shannon mappings for robust communication," *Telektronikk*, vol. 98, no. 1, pp. 114–128, 2002.

[15] F. Hekland, P. Floor, and T. A. Ramstad, "Shannon-Kotel'nikov mappings in joint source-channel coding," *IEEE Trans. Commun.*, vol. 57, no. 1, pp. 94–105, Jan 2009.

[16] G. de Oliveira Brante, R. Souza, and J. Garcia-Frias, "Analog joint source-channel coding in rayleigh fading channels," in *Proc. of Internation Conference on Acoustic, Speech and Signal Processing (ICASSP)*, May 2011, pp. 3148–3151.

[17] F. Vazquez-Araujo, O. Fresnedo, L. Castedo, and J. Garcia-Frias, "Analog joint source-channel coding over MIMO channels," *EURASIP Journal on Wireless Communications and Networking*, vol. 2014:25, no. 1, 2014.

[18] A. Lapidoth and S.Tingueley, "Sending a bivariate Gaussian over a Gaussian MAC," *IEEE Trans. Inform. Theory*, vol. 56, no. 6, pp. 2714–2752, 2010.

[19] M. S. Mehmetoglu, E. Akyol, and K. Rose, "Deterministic Annealing-Based Optimization for Zero-Delay Source-Channel Coding in Networks," *IEEE Trans. Commun.*, vol. 63, no. 12, pp. 5089–5100, Dec 2015.

[20] S. Yao and M. Skoglund, "Analog Network Coding Mappings in Gaussian Multiple-Access Relay Channels," *IEEE Trans. Commun.*, vol. 58, no. 7, pp. 1973–1983, July 2010.

[21] S. Shi, M. Schubert, and H. Boche, "Downlink MMSE Transceiver Optimization for Multiuser MIMO Systems: MMSE Balancing," *IEEE Trans. Signal Processing*, vol. 56, no. 8, pp. 3702–3712, Aug 2008.

[22] P. Suárez-Casal, O.Fresnedo, L. Castedo, and J. García-Frías, "Parametric analog mappings for correlated Gaussian sources over AWGN channels," in *2016 IEEE International Conference on Acoustics, Speech and Signal Processing (ICASSP)*, March 2016, pp. 3761–3765.

[23] C. Tian, S. Diggavi, and S. Shamai, "The achievable distortion region of sending a bivariate gaussian source on the gaussian broadcast channel," *IEEE Trans. Inform. Theory*, vol. 57, no. 10, pp. 6419–6427, Oct 2011.

[24] S. M. Kay, *Fundamentals of Statistical Signal Processing*. Prentice Hall, 1993.

[25] E. Akyol, K. Rose, and T. Ramstad, "Optimized analog mappings for distributed source-channel coding," in *Proc. of IEEE Data Compression Conference*, 2010.

[26] B. Lu and J. Garcia-Frias, "Non-linear bandwidth reduction schemes for transmission of multivariate Gaussian sources over noisy channels," in *Information Sciences and Systems (CISS), 46th Annual Conference on*, March 2012.

[27] M. Hassanin, J. Garcia-Frias, and L. Castedo, "Analog joint source channel coding for Gaussian Broadcast Channels," in *Acoustics, Speech and Signal Processing (ICASSP), 2014 IEEE International Conference on*, May 2014, pp. 4264–4268.

[28] O. Fresnedo, F. Vazquez-Araujo, L. Castedo, and J. Garcia-Frias, "Low-complexity near-optimal decoding for analog joint source channel coding using space-filling curves," *IEEE Commun. Lett.*, vol. 17, no. 4, pp. 745–748, Apr 2013.

[29] P. A. Floor, A. N. Kim, N.Wernersson, T. A. Ramstad, M. Skoglund, and I. Balasingham, "Zero-delay joint source-channel coding for a bivariate Gaussian on a Gaussian MAC," *IEEE Trans. on Comm.*, vol. 60, no. 10, pp. 3091–3102, Oct 2012.